Proceedings of the 17th World Congress
The International Federation of Automatic Control
Seoul, Korea, July 6-11, 2008

Defects Detection of Billet Surface Using Optimized Gabor Filters

Jong Pil Yun* SungHoo Choi* Boyeul Seo* Chang Hyun Park* Sang Woo Kim*

**Electronic and Electrical Engineering Department, Pohang University of Science and Technology, Pohang, Korea, (e-mail: {rebirth, csh425, boyeul80,chpark89, swkim}@postech.ac.kr)*

Abstract: This paper deals with a defects detection algorithm for billet surface. To get good performance, detection algorithm has to solve several difficult problems such as shape of a billet, many kinds of defects, much scale. Especially, the scale, that is a metallic oxide on steel surface, makes worse severely the performance of detection. To solve above problems, this paper presents a new effective defects detection algorithm based on Gabor filters optimized by Genetic Algorithm. The experimental results conducted on real billet surface images and demonstrate the good performance of the proposed algorithm.

Keywords: Defect detection, Gabor filter, Billet surface, Filter selection

1. INTRODUCTION

In steel manufacturing industry, it becomes significant to enhance quality of products as well as to increase quantity of products. The defects on the surface of billet affect quality of BIC (Bar in Coil), therefore on-line surface inspection is of great importance to improve quality of steel products. However, the quality assurance of a billet surface is still carried out by human operators. This manual inspection cannot cover overall surface of a billet. Due to the different criterion of inspectors, the reliability and the accuracy of this inspection cannot be guaranteed (Yun et al., 2006). So, in order to overcome manual inspection, many engineers concentrate on the automatic defects detection**.**

There have been various approaches for the defects detection in many kinds of manufacturing such as ceramic tiles (Elbehiery et al., 2005), rail surfaces (Deutschl et al., 2004), LCD(liquid Crystal Display) panel (Song et al., 2006), textured materials (Kumar et al., 2002 a), (Yang et al., 2005), (Cho et al. 2005), and so on. Although these methods have good performance in the respective industries, it is hard to apply these methods to billet surface directly because each target has different features.

Various approaches for defects detection have been proposed in steel manufacturing industry. The feed-forward neural network technique has been used to detect defects of cold rolled strips. The gray level arrangement of neighbor pixels was used to extract the feature vector (Kang et al., 2005). A hybrid image segmentation method based on corner detection and Fisher discriminant has been presented to detect surface defects of ship plate (Guo et al., 2006). The wavelet technique has been applied for defect detection of castings (Li et al., 2006). In a hot rolling process, a real-time visual inspection system that used support vector machine to automatically learn complicated defect patterns has proposed (Jia et al., 2004).

In addition, many other methods applied to detection of steel surface defects (Sugimoto et al., 1998), (Yun et al., 2006), (Choi et al., 2007). Although, these methods deals with steel products, it is hard to apply directly to billet defects detection since each methods are optimized on specific steel type, lightening, and manufacturing speed. Moreover, the billet surface is covered with a lot of scale. Although it does not affect the quality of the product, it makes difficult to distinguish scale from crack. In addition, scale of the billet has wide gray level range. These characteristics make it difficult to analysis image. So a new detection method which responds to only real defects, not scale is needed.

In this paper, we propose a novel defects detection algorithm based on Gabor filtering method for solving the problem of detecting defects in billet surface. In order to obtain optimized Gabor filters, GA (Genetic Algorithm) is used in this paper. And to remove noise still remained after binarizing, the morphological operation is used.

This paper is organized as follows: Section 2 analyzes intrinsic features of billet surface image. Section 3 presents defects detection algorithm based on the optimized Gabor filters in detail. The performance of the proposed defects detection algorithm is evaluated in Section 4. Finally, Section 5 gives conclusions.

2. ANALYSIS OF BILLET SURFACE IMAGE

Fig. 1(a) shows billets surface image which is our target of defects detection. The billet is in the form of long quadrangle stick. One of the four sides of billet is shown in Fig. 1(a). Fig. 1(b) shows gray level of a horizontal line from A to B in Fig. 1(a). The gray level of both right and left sides is different from center, because the billet has round corners not rectangular. There is a defect between 10-50 pixels of horizontal direction in Fig. 1. It is shown that the scale exists in not only defects parts but also all over the image. The scale is oxidized substance unavoidable caused during manufacturing process. The scale does not affect product quality, because it is eliminated during hot rolling process as a finished product process. But it makes difficult to detect defects, because the scale is mainly on the surface of billet.

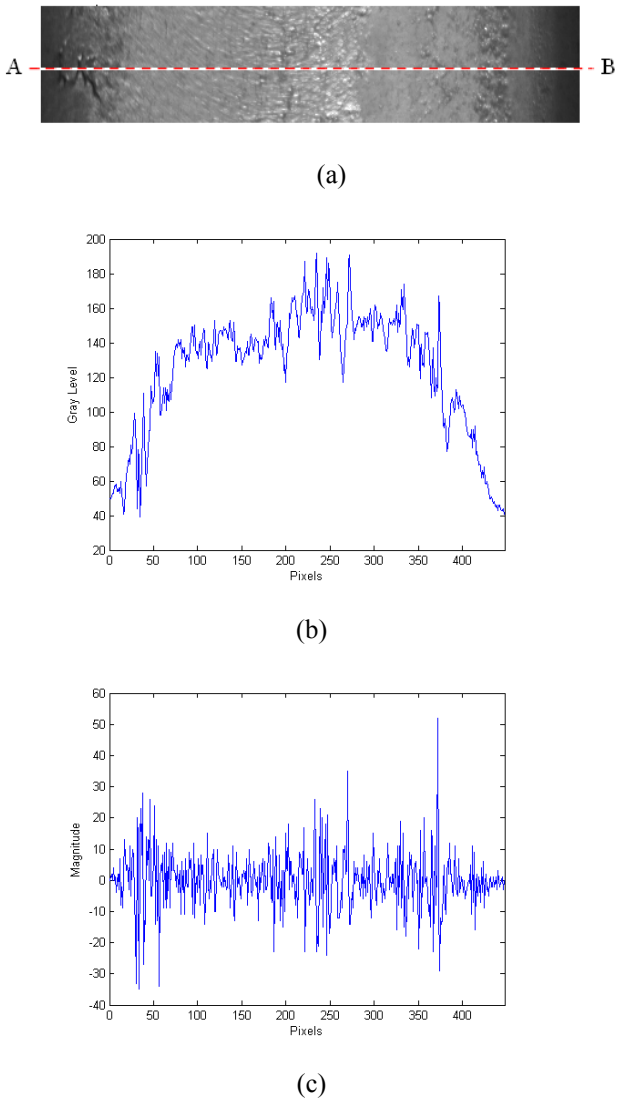

Fig. 1. Billet surface image with corner crack (a) original image (b) gray level of a horizontal line (c) 1st differential value of a horizontal line

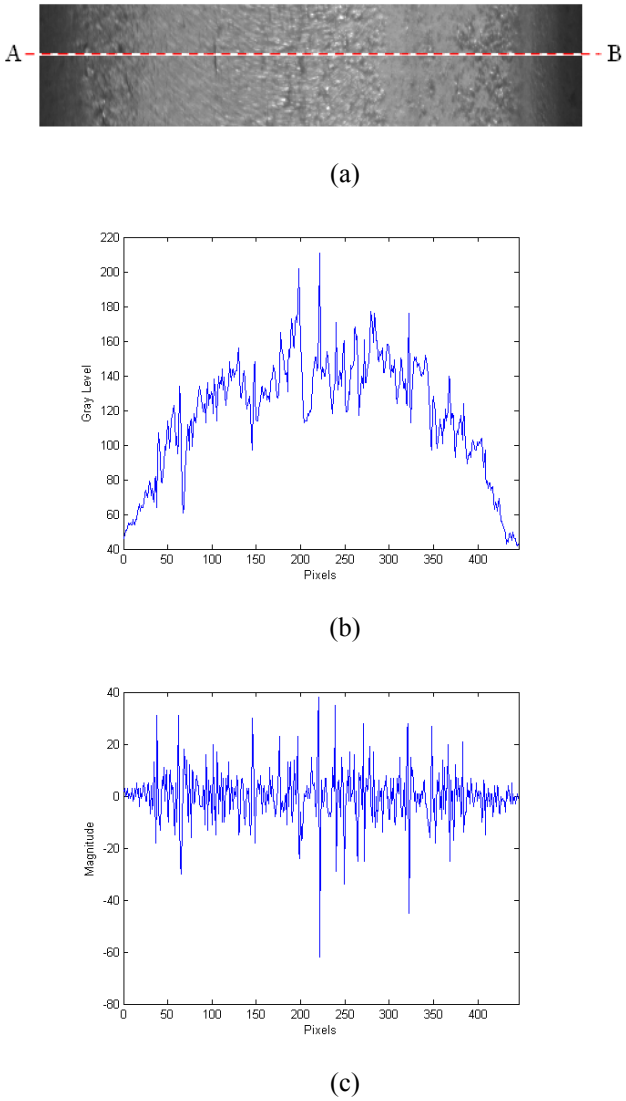

Fig. 2. Billet surface image with thin crack (a) original image (b) gray level of a horizontal line (c) 1st differential value of a horizontal line

The light can reflect off the scale part, which causes a very high gray level. On the other hand, it can also have a low gray level if the scale part comes out dark. If the scale has low gray level, it seems to be a defect. A defect exists between 140~150 pixels from left in Fig. 2. As shown is Fig. 2 (b), gray level of the defect is similar to scale.

The gradient magnitude of gray level is calculated to analyze the image in greater detail. The gradient value of horizontal direction can be expressed like as follows:

$$D(x, y) = I(x, y) - I(x-1, y) \qquad (1)$$

where x and y are the spatial indies. $I(x, y)$ is input image and $D(x, y)$ is first-order derivative. The gradient information using (1) is shown in Fig. 1(c) and Fig. 2(c). Not only defects but also scale has high gradient magnitude. This causes serious difficulty in the threshold level decision which discriminated between the defect the scale. Therefore, a new algorithm for billet images must have ability to detect only defects among defects and scale.

In this paper, we present the technique focused on crack which has a huge effect on the product quality. The crack divided into two classes. As shown in Fig. 1, the first thing is located at right or left side of the image. The sizes are comparatively big, and the shapes are various. And a gray level of defects is low. We named this crack for corner crack. The corner crack is generated by rolling process, which is pre-processing of BIC process. The other thing is detected mainly in the middle part of an image, the width is very thin, typically 1~2 pixels. In this paper, this crack is called the thin crack. Because the gray level of thin crack is similar to that of scale, it is so difficult to distinguish crack from scale. To solve above problems, we propose effective defects detection algorithm. In this paper, defects detection of billet surface using optimized Gabor filters is investigated. Gabor filters have been widely used in image processing and analysis. An

important property of Gabor filters is that they achieve maximum possible joint localization, or resolution in both spatial and spatial-frequency domain. In spatial domain a Gabor function is modulation product of complex exponential and a Gaussian envelope of arbitrary duration, in frequency it is seen as a shifted Gaussian (Shu et al., 2004). Gabor filters can decompose the image into components corresponding to different scales and orientation, therefore, have been used extensively for texture analysis, document analysis, object detection, and so on (Kumar., 2002 a). The proposed defects detection algorithm of billet surface using optimized Gabor filters is explained in next session.

3. PROPOSED DEFECTS DETECTION ALGORITHM

3.1 Gabor Function

A two-dimensional Gabor function consists of a sinusoidal plane wave of some frequency and orientation, modulated by a two-dimensional Gaussian envelope. In order to conveniently find a local spectral component of a texture, the real part of a Gabor function is used (Mak et al., 2005 a). In general, a two-dimension real part of a Gabor function $g(x, y)$ has the following general form:

$$g(x,y) = \exp\left[-\frac{1}{2}\left\{\left(\frac{x'}{\sigma_x}\right)^2 + \left(\frac{y'}{\sigma_y}\right)^2\right\}\right]\cos(2\pi f x') \qquad (2)$$

where

$$x' = x\cos\theta + y\sin\theta$$
$$y' = -x\sin\theta + y\cos\theta,$$

θ denotes the rotation parameter, f is the radial frequency of the Gabor function. The space constants σ_x and σ_y define the Gaussian envelope along the x and y axes. For a given input image $I(x, y)$, the new image $R(x, y)$ is obtained by using Gabor filter $g(x, y)$ as follows:

$$\begin{aligned} R(x,y) &= g(x,y) * I(x,y) \\ &= \sum_{m=0}^{M-1}\sum_{n=0}^{N-1} g(m,n) I(x-m, y-n) \end{aligned} \qquad (3)$$

where m, n are the Gabor filter mask size variables, and (*) denotes the 2-D convolution. The squaring nonlinear operator $|\cdot|^2$ computes the energy of every pixel in the filtered image $R(x, y)$:

$$E(x,y) = R^2(x,y). \qquad (4)$$

In this paper, the objective of Gabor filter $g(x,y)$ is to maximize the difference between energy of the defect-free billet surface and billet surface with defect.

3.2 Optimized Filter Selection

The Gabor filter has different response in the spatial and the frequency domains according to four parameters such as σ_x, σ_y, f, and θ. Also as the parameters of Gabor filter change, the energy response $E(x, y)$ of input image $I(x, y)$ changes. Therefore the choice of Gabor filter parameters is crucial role in the defects detection application.

Our goal is to detect defects by enlarging the difference of energy response between the defects and defect-free. Therefore, two cost functions using the energy mean are presented to find the optimum parameters of Gabor filter in this paper. And the optimized Gabor filter is determined by genetic algorithm which searches maximum value of cost function related energy separation criteria.

The following mean μ are used to represent the feature of the image.

$$\mu = \frac{1}{P \times Q}\sum_{(x,y)\in \text{region}} E(x,y). \qquad (5)$$

P and Q is size of given image. The first cost function is represented by ratio between the energy of defect image and defect-free image with scale as follows (Kumar et al., 2006 b):

$$J_1 = \frac{\mu_f}{\mu_d} \qquad (6)$$

Where μ_d is the average energy of image with defect and μ_f is the average energy of defect-free image with scale. The Gabor filter $g(x, y)$ that gives the highest cost function J_1 is chosen as the best effective filter to detect defects. If Gabor filter which is determined by using J_1 apply to image with defects, the energy should be low, i.e., low μ_d. On the contrary, the response of defects-free image with scale should be strong, i.e., high μ_f.

The second cost function J_2 is designated as normalized difference of μ_d and μ_f

$$J_2 = \frac{|\mu_d - \mu_f|}{\mu_f}. \qquad (7)$$

In contrast to J_1, the second cost function J_2 increases along with μ_d increases. On the other hand, the smaller μ_f is, the higher value of J_2 becomes.

In order to obtain optimized Gabor filter which makes maximum value J_1 or J_2, genetic algorithm is used in this paper. Because genetic algorithm searches the minimum value of the fitness function, the reciprocal of J is adopted. The chromosome vector is as follows:

$$C = [\sigma_x \ \ \sigma_y \ f \ \ \theta] \qquad (8)$$

The population size is 100. The selection, reproduction, crossover and random mutation are efficiently implemented. The mutation operation changes one of the parent based on a uniform probability distribution. Because of constraints of computational simplicity, the size of Gabor masks is limited

to 9×9. Therefore, σ_x and σ_y is limited to 0.001-4.999. The radial frequency f is limited 0-32 heuristically. Finally, θ lies between 0-2π.

3.3 Thresholding and Binarizing

The thresholding process discriminates between image with defects and defects-free image with scale. It process is applied to $R(x, y)$ passed through optimized Gabor filter. In order to select optimal threshold value, a defect-free image sample is used to generate a filtered image $R(x, y)_f$. From this filtered image, the threshold value related to J_1 is obtained as follows:

$$T_1 = \alpha \times \min_{x,y \in W} \{R(x,y)_f\}, \tag{9}$$

where α is the weighting factor determined by the experiment. W is a window centered at the image $R(x, y)_f$. The window size is chosen to avoid the possible undesirable effects due to border distortion (Kumar et al., 2002 a). A binary algorithm is represented as follows

$$\begin{aligned} &\text{if } T_1 > R(x,y) \text{ then } BI(i,j) = 1 \\ &\text{else } BI(x,y) = 0 \end{aligned} \tag{10}$$

where $BI(x, y)$ is a binary image changed by the threshold value T_1. In the binary image, the value of 1 means defects, and 0 means defect-free. On the other hand, because J_2 has maximum value at high μ_d, T_2 related to J_2 has different value against T_1. The thresholding value T_2 related to J_2 is obtained as follows:

$$T_2 = \beta \times \max_{x,y \in W} \{R(x,y)_f\}, \tag{11}$$

where β is the weighting factor. And binary algorithm for T_2 is represented as follows

$$\begin{aligned} &\text{if } T_2 < R(x,y) \text{ then } BI(i,j) = 1 \\ &\text{else } BI(x,y) = 0. \end{aligned} \tag{12}$$

3.4 Morphological Operation

To remove small noise still remained after binarizing, morphological technique is used. Erosion and dilation are the most basic morphological operators, which can serve as the fundamental elements in the expressions of other complicated operators (Mak et al., 2005 b).

The dilation of A by B, denoted $A \bigcirc B$, is defined as

$$A \bigcirc B = \{z \mid (B^*)_z \bigcap A \neq \varnothing\}. \tag{13}$$

The dilation of A by B then is the set of all displacements, z, such that B and A overlap by at least one element (Gonzalez et al., 2002). The reflection of set is denoted B^* is defined as

$$B^* = \{w \mid w = -b, \text{ for } b \in B\}. \tag{14}$$

The translation of set A by point $z=(z_1+z_2)$, denoted $(A)_z$, is defined as

$$(A)_z = \{c \mid c = a + z, \text{ for } a \in A\}. \tag{15}$$

The erosion of A by B, denoted $A \odot B$, is defined as

$$A \odot B = \{z \mid (B)_z \subseteq A\}. \tag{16}$$

In words, this equation indicates that the erosion of A by B is the set of all points z such that B, translated by z, is contained in A (Gonzalez et al., 2002). When an image is eroded or dilated by a structuring element, some information in the original image will be lost. In order to recover the lost information caused by erosion, dilation and to remove small noise in the $B(x, y)$, opening operation and closing operation are adopted. The opening of set A by structuring element B, denoted $A \bullet B$, is defined as

$$A \bullet B = (A \bigcirc B) \odot B. \tag{17}$$

And the closing operation is defined as follow:

$$A \circ B = (A \odot B) \bigcirc B. \tag{18}$$

Thus, the opening A by B is the erosion of A by B, followed by a dilation of the result by B. On the other hand, the closing operation is a contrary concept of the opening operation. The structuring element B influences the elimination rates of noise. Therefore, selection of the structuring element B is very important. And also, the size of structuring element B influences the calculation speed. Hence, a structuring element is decided on by the maximum size of a noise and minimum size of a defect (Cho et al., 2005). Based on the analysis results of corner crack and thin crack, the opening operation mask $B_1=[1\ 1\ 1]^T$ and the closing operation mask $B_2=[1\ 1\ 1]^T$ are used for corner crack. The opening operation mask $C_1=[1\ 1\ 1\ 1\ 1\ 1\ 1]^T$ and the closing operation mask $C_2=[1\ 1\ 1\ 1\ 1\ ]^T$ are applied to thin crack.

4. EXPERIMENT AND RESULTS

To evaluate the performance of the proposed detection algorithm, we used the billet images directly acquired from the real production line. The size of images is 1024 by 1000. The parameters of optimized Gabor filters are determined by the (6) and (7) for the corner crack and thin crack respectively. To search maximum value of the each cost function (6) and (7), the genetic algorithm is used. In the experiment results, Equation (6) is suitable for separating defect region and defect-free region for billet image with corner crack. On the contrary, (7) is fit for thin crack. The parameters of the Gabor filters optimized by genetic algorithm is shown in Table 1. Fig. 3(a) and (b) illustrate the optimized Gabor filters for corner crack and thin crack respectively. The performance of the proposed detection algorithm is evaluated by using 370 real billet images in which

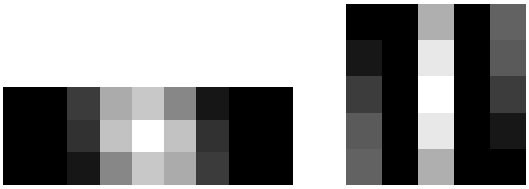

(a) (b)

Fig. 3. Optimized gabor filters (a) for corner crack (3×9) (b) for thin crack (5×5)

Table 1. Gabor filter parameters obtained by the optimized filter selection method

	σ_x	σ_y	f	θ *(radian)*
Corner crack	1.4418	4.6364	9.0806	3.0193
Thin crack	2.69462	2.23709	14.1081	5.89016

192 images are defect-free and the rest is with defects. The test results are summarized in Table 2. The proposed algorithm has 91.13% and 83.83% accuracy for corner crack and thin crack respectively. Some of the detection results for the billet image are presented in Fig. 4-8. Fig. 4-6 are the results for the image with corner crack and Fig. 7 show the results for thin crack. On the other hand, Fig. 8 shows the results for a billet image with scale. Each (b) in Fig. 4-8 are images passed through the optimized Gabor filters and each (c) is binary image obtained after thresholding operation. Final results after noise removal using morphological operation are shown in Fig 4-8 (d). Especially as shown Fig. 8 (d), the scale which seems to be defects is not detected. Consequently, the proposed defects detection algorithm using optimized Gabor filters is effective for billets surface image with scale.

5. CONCLUSIONS

In this paper, a new defect detection algorithm based on the optimized Gabor filters for billet surface is presented. The billet surface image has a lot of scale which is oxidized substance unavoidably caused during manufacturing process and extensions. Because scale of billet surface is similar to real defects such as crack, it is difficult to distinguish defects from image with scale. To solve this problem, we propose optimization approaches utilizing energy separation criteria. The optimized Gabor filter is determined by genetic algorithm which searches maximum value of cost function related energy separation criteria. The image, which is passed through the optimized Gabor filters, changes to binary image using thresholding. To remove small noise still remained after binarizing, morphological technique is used. In this paper, two structuring element filters proposed for each defects. To evaluate the performance of the proposed algorithm, the detection efficiency is measured by experiment using the real billet image. Experiment results show that the proposed algorithm is effective and suitable for billet image with scale.

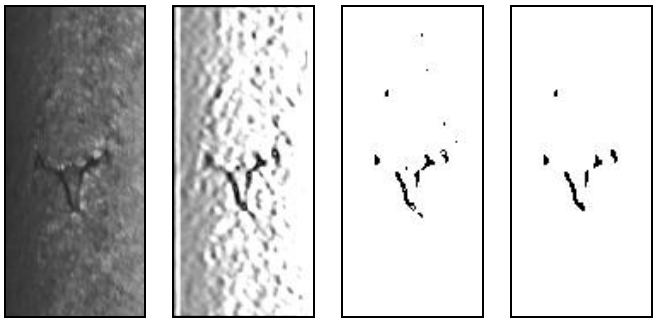

(a) (b) (c) (d)

Fig. 4. Example 1 for detection results of corner crack (a) Gray-level billet image (b) Filtered image (c) Binary image obtained as a result of thresholding (d) Result image obtained after morphological operation

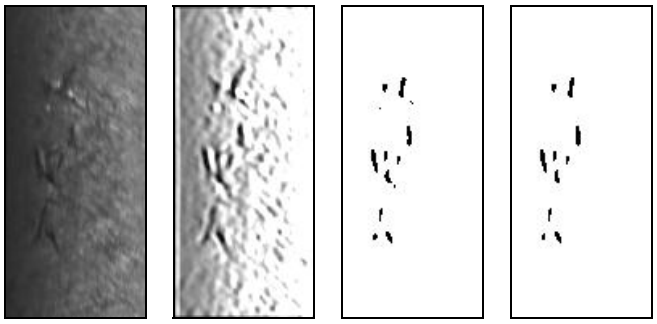

(a) (b) (c) (d)

Fig. 5. Example 2 for detection results of corner crack (a) Gray-level billet image (b) Filtered image (c) Binary image obtained as a result of thresholding (d) Result image obtained after morphological operation

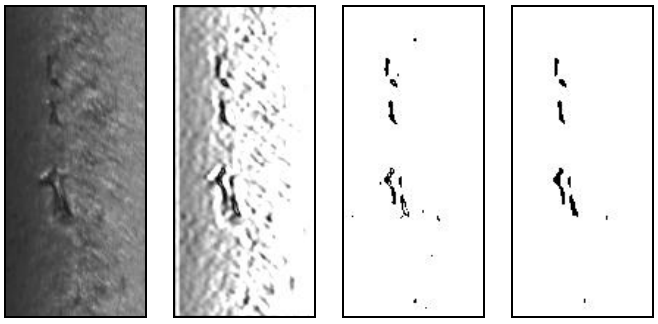

(a) (b) (c) (d)

Fig. 6. Example 3 for detection results of corner crack (a) Gray-level billet image (b) Filtered image (c) Binary image obtained as a result of thresholding (d) Result image obtained after morphological operation

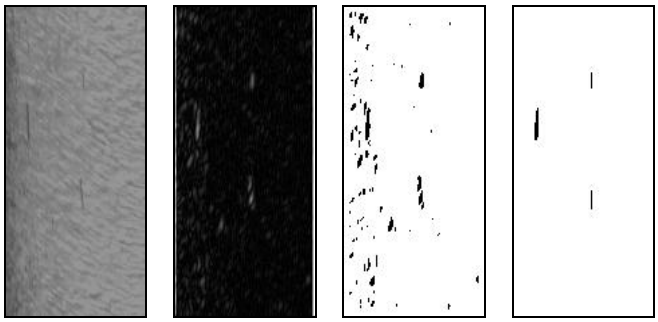

(a) (b) (c) (d)

Fig. 7. Example for detection results of thin crack (a) Gray-level billet image (b) Filtered image (c) Binary image obtained as a result of thresholding (d) Result image obtained after morphological operation

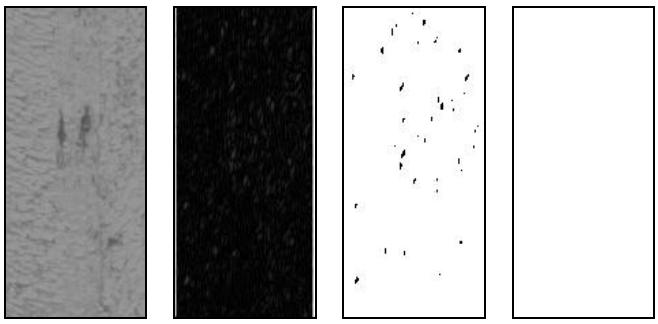

(a) (b) (c) (d)

Fig. 8. Example of detection results of image with scale (a) Gray-level billet image (b) Filtered image (c) Binary image obtained as a result of thresholding (d) Result image obtained after morphological operation

Table 2. The experiment results of the proposed detection algorithm

	Defects		Non-defects		accuracy
	success	fail	success	fail	
Corner crack	98	10	87	8	91.13%
Thin crack	56	14	84	13	83.83%

REFERENCES

C. -S. Cho, B. -M. Chung, and M. -J. Park (2005). Development of Real-Time Vision-Based Fabric Inspection System. *IEEE Trans. Industrial Electronics,* **52** No. 4**,** 1073-1079.

S. H. Choi, J. P. Yun, B. Seo, Y. S. Park, and S. W. Kim (2007). Real-time Defects Detection Algorithm for High-speed Steel Bar in Coil. *Enformatika Trans. on Engineering, Computing and Technology*, **19**, 66-70.

E. Deutschl, C. Gasser, A. Niel, and J. Werschonig (2004). Defect Detection on Rail Surfaces by a Vision based System. *IEEE Intelligent Vehicles Symposium*, 507-511.

H. Elbehiery, A. Hefnawy, and M. Elewa (2005). Surface Defects Detection for Ceramic Tiles Using Image Processing and Morphological Techniques. *IEEE Trans. Engineering, Computing and Technology*, **5**, 158-162.

R. C. Gonzalez, R. E. Woods (2002). *Digital Image Processing*. Chapter 9, Prentive-Hall, Upper Saddle River, New Jersey.

J. H. Guo, X. D. Meng, and M. D. Xiong (2006). Study on Defection Segmentation for Steel Surface Image Based on Image Corner Detection and Fisher Discriminant. *Journal of Physics: Conf. Series 48*, 364-368.

H. Jia, Y. L. Murphey, J. Shi, and T. –S. Chang (2004). An Intelligent Real-time Vision System for Surface Defect Detection. *Proceedings of the International conference on Pattern Recognition.*, **3**, 239-242.

G.- W. Kang, H. -B. Liu (2005). Surface Defects Inspection of Cold Rolled Strips Based on Neural Network. *Proc. International Conference on Machine Learning and Cybernetics*, **8**, 5034-5037.

A. Kumar, G. K. H. Pang (2002)a. Defect Detection in Textured Materials Using Gabor Filters. *IEEE Trans. Industry Applications*, **38** No. 2, 425-440.

A. Kumar, G. K. H. Pang (2002)b. Defect Detection in Textured Materials Using Optimized Filters. *IEEE Trans. System, Man, Cybernetics*, **32** No. 5, 553-570.

X. Li, S. K. Tso, X.-P. Guan, Q. Huang (2006). Improving Automatic Detection of Defects in Castings by Applying Wavelet Technique. *IEEE Trans. Industrial Electronics*, **53** No. 6, 1927-1934.

K. L. Mak, P. Peng, and H. Y. K. Lau (2005)a. A Real- time Computer Vision System for Detecting Defects in Textile Fabrics. *IEEE International Conference on Industrial Technology*, 469-474.

K. L. Mak, P. Peng, H.Y,K. Lau (2005)b. Optimal Morphological Filter Design for Fabric Defect Detection. *IEEE International Conference on Industrial Technology*, 799-804.

Y. Shu, and Z. Tan (2004). Fabric Defects Automatic Detection Using Gabor Filters. *Proc. World Congress on Intelligent Control and Automation*, **4**, 3378-3380.

Y.- C. Song, D.- H. Choi, K.- H. Park (2006). Wavelet-Based Image Enhancement for Defect Detection in Thin Flim Transistor Liquid Crystal Display Panel. *Japanese Journal of Applied Physics*, **45** No. 6A, 5069-5072.

T. Sugimoto, T. Kawaguchi (1998). Development of a Surface Defect Inspection System Using Radiant Light from Steel Products in a Hot Rolling Line. *IEEE Trans. Instrumentation and Measurement*, **47** No. 2**,** 409-416.

X. Yang, G. Pang, and N. Yung (2005). Robust Fabric defect detection and classification using multiple adaptive wavelets. *IEE Proc.-Vision, Image and Signal Processing,* **152** No. 6, 715-723 .

J. P. Yun, Y. S. Park, B. Seo, S. W. Kim, S. H. Choi, C. H. Park, H. M. Bae, and H. W. Hwang (2006). Development of Real-time Defect Detection Algorithm for High-speed Steel Bar in Coil(BIC). *SICE-ICASE International Joint Conference*, 2495-2498.